






Article

An Insight into the Reactivity of the Electrogenerated Radical Cation of Caffeine

Marta Feroci ¹, Martina Bortolami ¹, Isabella Chiarotto ¹, Paola Di Matteo ²,
Leonardo Mattiello ¹, Fabiana Pandolfi ¹, Daniele Rocco ¹ and Rita Petrucci ^{1,*}

¹ Dipartimento di Scienze di Base e Applicate per l'Ingegneria (SBAI), Sapienza University of Rome, 00161 Roma, Italy; marta.feroci@uniroma1.it (M.F.); martina.bortolami@uniroma1.it (M.B.); isabella.chiarotto@uniroma1.it (I.C.); leonardo.mattiello@uniroma1.it (L.M.); fabiana.pandolfi@uniroma1.it (F.P.); daniele.rocco@uniroma1.it (D.R.)

² Dipartimento di Ingegneria Chimica, Materiali e Ambiente, Sapienza University of Rome, 00184 Rome, Italy; p.dimatteo@uniroma1.it

* Correspondence: rita.petrucci@uniroma1.it; Tel.: +39-06-4976-6736

Received: 10 February 2020; Accepted: 9 March 2020; Published: 12 March 2020



Abstract: Controlled potential electrolyses of caffeine (CAF) were carried out at a Pt electrode in undried acetonitrile (ACN) and ACN-H₂O and the products of the anodic oxidation were analyzed by HPLC-PDA-ESI-MS/MS. A higher current efficiency occurred in ACN-H₂O, but an analogous chromatographic outline was found in both media, evidencing a reactive pathway of the electrogenerated radical cation CAF^{•+} with water, added or in trace, as nucleophile. No dimeric forms were evidenced, excluding any coupling reactions. Neither was 1,3,7-trimethyluric acid found, reported in the literature as the main oxidative route for CAF in water. Four main chromatographic peaks were evidenced, assigned to four proposed structures on the base of chromatographic and spectral data: a 4,5-diol derivative and an oxazolidin-2-one derivative were assigned as principal oxidation products, supporting a mechanism proposed in a previous work for the primary anodic oxidation of the methylxanthines olefinic C⁴ = C⁵ bond. Two highly polar degradation products were also tentatively assigned, that seemed generating along two different pathways, one opening the imidazolic moiety and another one opening the purinic one.

Keywords: caffeine; anodic oxidation; HPLC-PDA-ESI-MS/MS; oxidative stress; antioxidant capacity

1. Introduction

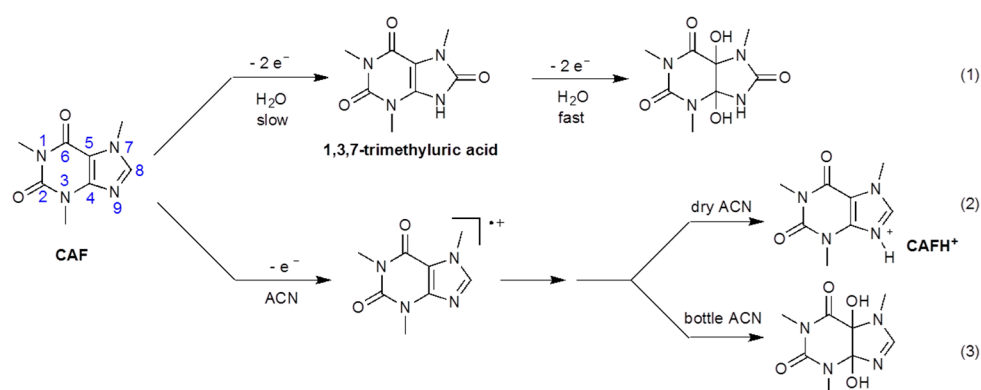
The widespread natural caffeine (1,3,7-trimethylxanthine, CAF, Scheme 1), taken daily with the diet as an important component of highly popular beverages as coffee and tea, has been widely studied for decades. Many systemic and physiological effects of CAF in humans are well known, and some therapeutic properties have been used in medicine for different pathologic contexts, such as respiratory disease and cardiovascular disease [1–6]. Beneficial health effects have been more recently proposed on obesity and diabetes, fertility, and neurodegenerative disease as Alzheimer's and Parkinson's disease; in these last cases the proper mechanism of caffeine-induced protection has not been fully clarified yet. Some detrimental effects also suggested an intrinsic complexity and concern due to the wide consumption [7]. A protective effect towards oxidative damage has been supported by in vitro and in vivo experiments [8–10], and a possible antioxidant ability of CAF has been studied [11,12], the role of CAF remaining nevertheless an open discussion.

CAF has been also investigated for synthetic applications in the sustainable pharmaceutical chemistry. In fact, the xanthine structural core of CAF represents a useful natural renewable starting material in the synthesis of known and/or new drugs, especially addressed to diseases related to

oxidative stress [13–16]. Because of its high chemical stability, CAF needs drastic conditions to react, while an easier reactivity is shown by electrochemical route. In this regard, the electrochemical reduction of CAF in organic solvent has been recently reported, the methodology leading to an amino-functionalized imidazole, not chemically obtainable, with valuable applications in organic synthesis [17,18]. It is in fact well known that in some cases electrochemistry can lead to different products than those obtained by classical chemical reactions [19].

A larger number of reports are available in literature regarding the electrochemical oxidation of CAF that occurs quite easily if compared to the electrochemical reduction. The great interest in the analyte CAF, present in many beverages and drug formulations among the most consumed products all over the world [20], continuously encourages the research in the analytical field, where electrochemical methods based on the anodic oxidation of CAF at a multitude of different electrode materials and nanomaterials join more conventional methods [21–25].

Although CAF presents both hydrophilic and lipophilic properties, the caffeine electrochemical oxidation has been reported mainly in aqueous medium, where an irreversible four electrons process has been found and a pathway involving a slow first oxidation to trimethyluric acid followed by a fast formation of the corresponding 4,5-diol derivative, has been proposed (Scheme, Equation (1)) [26,27]. Various mechanisms have been proposed also for the chemical oxidation of CAF by radical species differently generated, water being the medium [28,29].



Scheme 1. Proposed oxidation mechanisms in literature: (1) [26,27]; (2) [30]; (3) [31].

Only two studies, at least up to our knowledge, have been reported on the electrochemical oxidation of CAF in non-aqueous medium, both evidencing a mono-electronic first oxidation process leading to a radical cation [30,31]. A different fate was predicted for the electrogenerated CAF^{•+}: a reaction with a hydrogen atom donor was proposed in a strongly dry acetonitrile to give the diamagnetic cation CAFH⁺, the last one evidenced by comparison with the chemical oxidation product (Scheme, Equation (2)) [30], and a quite stable radical cation was proposed in anhydrous acetonitrile as a substrate available for a following nucleophilic attack to give 4,5-saturated derivatives (Scheme, Equation (3)) [31]. A different behavior has been proposed for the radical cation obtained by the electrochemical oxidation of theophylline (1,3-dimethylxanthine, TPh) in anhydrous acetonitrile, suggesting a fast deprotonation of TPh^{•+} and 8-substituted derivatives as final oxidation products [31]. The anodic oxidation of TPh in organic solvents, also in the presence of equimolar amount of water, has been recently reported and dimers of TPh as 8-substituted oxidation products as well as 4,5-disubstituted derivatives have been evidenced [32].

In the present work, the electrochemical oxidation of CAF was carried out in acetonitrile, considered a good environment to investigate radical species, and in aqueous acetonitrile, to provide a controlled amount of water as nucleophilic reactant. The oxidation products were analyzed by HPLC-PDA-ESI-MS/MS, with the aim to investigate on the nature and the reactivity of the radical cation of caffeine and shed light on a current topic as the behavior of caffeine under oxidative conditions in lipophilic environment.

2. Materials and Methods

2.1. Materials

All reagents (Sigma-Aldrich) and HPLC grade acetonitrile (Carlo Erba) were used as received. Et_4NBF_4 was kept at reduced pressure at 70 °C for 24 h before the use; HPLC grade water was obtained with the Milli-Q purification system (Millipore).

2.2. Cyclic Voltammetry

Voltammetric measurements were carried out on an Amel 552 potentiostat, an Amel 566 function generator, an Amel 563 multipurpose unit, and an Amel 863 recorder, using a cell equipped with three electrodes; CorrWare and CorrView for Windows version 2.8d1 Scribner were the acquisition and elaboration softwares. A glassy carbon (GC, Amel 492/GC/3) microelectrode was used, a Pt wire as counter electrode and as reference a modified saturated calomel electrode (mSCE: SCE with organic solvent junction; the oxidation peak potential of ferrocene on GC electrode in DMF-0.1M Et_4NBF_4 is $E_{\text{oxFc}} = +0.512$ V vs. mSCE). Scan rate: $\nu = 0.200$ Vs⁻¹. All cyclic voltammetries were recorded at room temperature on 5 mL of solvent/0.1 M Et_4NBF_4 .

2.3. Controlled Potential Electrolysis

Controlled potential electrolyses were performed at constant potential ($E = +1.85$ V, vs. SCE), at room temperature, in N_2 atmosphere, with an Amel Model 552 potentiostat and an Amel Model 731 integrator. All electrolyses were performed in a home-made divided glass cell (previously described [33]). A porous glass plug filled up with a layer of gel (i.e., methyl cellulose 0.5% vol in DMF-0.1 M Et_4NBF_4) was the separator; Pt spirals (apparent area 0.8 cm²) were used as both cathode and anode. Anolyte: 0.10 mmol of caffeine in 5 mL of CH_3CN -0.1 M Et_4NBF_4 with or without 1 eq of H_2O . Catholyte: 2 mL of CH_3CN -0.1 M Et_4NBF_4 . After 12 C (corresponding to 1 F), the anolyte was sampled and analyzed. After 25 C (corresponding to 2 F) the flow of current was stopped, and the anolyte was analyzed.

2.4. HPLC-PDA-ESI-MS/MS Analysis

HPLC separation was performed by a 1525 μ Waters module (Milford), on a Waters XBridge C18 (150 \times 2.1 mm i.d.) 5 μ m analytical column. The elution gradient, with a flow rate of 0.20 mL min⁻¹, was: 0–20 min, 5%–60% B; 20–40 min, 60% B; 40–42 min, 60%–5% B; 42–62 min, 5% B, where A was water/formic acid 0.02% and B was acetonitrile/formic acid 0.02%.

A detector Waters 996 photodiode array (PDA) was set for recording one spectrum per second in the 200–800 nm range, and a Quattro Micro Tandem MS-MS detector with an electrospray ionization (ESI) source Waters (Micromass) was set for acquiring full scan data in positive (pESI) and negative (nESI) modes, in the mass range 140–500 Da. ESI source parameters: capillary voltage 3000 V, cone voltage 25 V, source temperature 120 °C, desolvation temperature 350 °C, cone gas flow 40 L h⁻¹, desolvation gas flow 600 L h⁻¹.

The same instrument was used for infusion experiments in pESI and nESI modes, carried out in daughter mode; collision gas: argon. Direct infusion of samples into the source using an external syringe pump with a set flow rate of 5 μ L min⁻¹ was carried out; for each analyzed mass the parent ion and optimized collision energy (CE) value to obtain the best fragmentation pattern were selected. In detail: $[\text{M}+\text{H}]^+ = 229.10$ m/z CE 12 eV and 25 eV; $[\text{M}+\text{H}]^+ = 251.22$ m/z CE 12 eV and 15 eV; $[\text{M}+\text{Na}]^+ = 211.06$ m/z CE 15 eV and 18 eV and $[\text{M}-\text{H}]^- = 187.09$ m/z CE 15 eV and 16 eV; $[\text{M}-\text{H}]^- = 212.03$ m/z CE 12eV and 16 eV.

MassLynx Software 4.1 v (Data Handling System for Windows, Micromass) allowed data acquisition and handling and instruments control.

Samples dilution of the electrolyzed solution was 1:100 with mobile phase A/B (95:5, v:v); 20 μL of the filtrate was injected for the analysis (Cronus Syringe Filter 0.45 μm). The samples were analyzed at least in duplicate in independent runs.

The $[\text{M}+\text{H}]^+$ and/or $[\text{M}-\text{H}]^-$ m/z values of CAF and main oxidation products were extracted from the pESI and/or nESI Total Ion Chromatograms (TIC), the resulting pure peaks were integrated, using areas for current efficiency/yield calculation.

3. Results

3.1. Anodic oxidation of CAF

Cyclic voltammetry of CAF was carried out at a GC and Pt electrodes in acetonitrile (ACN) in the absence and in the presence of controlled amount of added water, at the scan rate of 0.200 Vs^{-1} . An irreversible anodic peak was observed at the potential value E_{ap} of +1.87 V vs. mSCE on GC electrode, with a slight anodic shift to +1.92 V observed after the addition of 1 equivalent of water. The same behavior was obtained on Pt electrode (see CV curves in Supplementary Material). Furthermore, an increase of the peak current density was observed in the presence of added water, doubling the starting peak current value ($I = 6.6 \times 10^{-4} \text{ A cm}^{-2}$ in ACN and $I = 1.4 \times 10^{-3} \text{ A cm}^{-2}$ in the presence of 1 equivalent of water). Electrochemical data are resumed in Table 1. Cyclic voltammograms without and with added water are shown in Figure 1, left and right, respectively (red curves).

Table 1. Cyclic voltammetric data of CAF at a GC working electrode in ACN without and with 1 equivalent of added water at the scan rate of 0.200 Vs^{-1} .

	ACN	ACN/1eq H_2O
E_{ap} (V) ^a	+1.87	+1.92
I (A cm^{-2}) ^b	6.64×10^{-4}	1.4×10^{-3}
$I_{2\text{F}}/I_0$ ^c	42%	14%

^a values are vs. mSCE; ^b I = current density; ^c I_0 = CAF CV peak current density value before electrolysis, $I_{2\text{F}}$ = CAF CV peak current density value after 2 F electrolysis

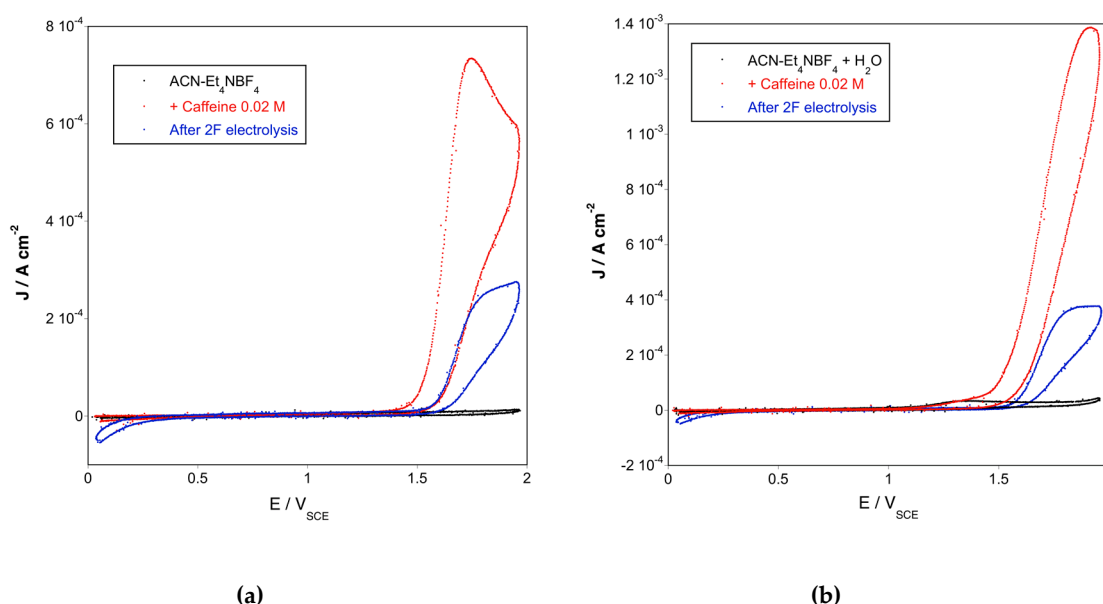


Figure 1. Cyclic voltammograms of caffeine (CAF) in undried acetonitrile (ACN) (left) and in ACN with 1 equivalent of added water (right), at a glassy carbon (GC) electrode, vs. modified saturated calomel electrode (mSCE), scan rate 0.200 Vs^{-1} : ACN/ $0.1 \text{ M Et}_4\text{NBF}_4$ (black lines); CAF 0.02 M in ACN/ Et_4NBF_4 (red lines); CAF in ACN/ Et_4NBF_4 after 2 F anodic oxidation (blue lines). (a) CV in undried ACN; (b) CV in ACN with added water.

The observed behavior was in agreement with data previously reported in the very few works on the electrochemistry of CAF in organic solvent [30,31] that supported the one electron first anodic oxidation of CAF to the corresponding radical cation. The increase of the peak current density in the presence of added water might be ascribed to the reactivity of the electrogenerated radical cation towards water, as previously reported [31].

To investigate on the fate of the radical cation of CAF, controlled potential electrolyses of CAF were carried out in ACN without and with added water, at the constant potential E of +1.85 V vs. SCE, on a Pt electrode, under a nitrogen atmosphere and at room temperature.

The electrolyzed solutions were analyzed after a controlled current consumption, corresponding to one Faraday (1 F) and two Faradays (2 F), respectively, by cyclic voltammetry and chromatographic separation followed by UV-vis spectrophotometric and mass spectrometric detection.

Cyclic voltammograms recorded on the electrolyzed solutions after 2 F electrolysis are shown as blue curves in Figure 1.

A higher current efficiency was found when the electrolysis was carried out in the presence of 1 equivalent of added water, as evidenced by the strong decrease of the anodic peak of CAF after 2 F electrolysis (Figure 1 right, blue curve): the ratio between the peak current density I measured after 2 F electrolysis (I_{2F}) and that one measured before starting the electrolysis (I_0) evidenced a 14% of the starting material left, versus a 42% evidenced in the electrolysis carried out without added water (Figure 1 left, blue curve). Data are resumed in Table 1.

The electrolyzed solutions were then analyzed by HPLC-PDA-ESI-MS/MS in order to get structural information on the oxidation products.

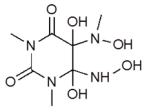
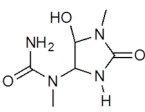
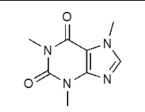
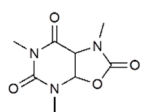
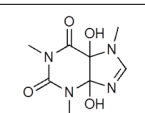
3.2. HPLC-PDA-ESI-MS/MS Analysis of Oxidation Products

Aliquots of the electrolyzed solutions were diluted 1:100 with mobile phase A/B (95:5, v:v), filtered and injected for the analysis.

The PDA chromatogram evidenced a similar profile for electrolyzed solution in ACN without and with added water, as shown in Figure S1 (Supplementary Materials), a and b, respectively. Four main peaks can be observed there: one at retention time (RT) 5.39 min was assigned to CAF by comparison with the starting material, one peak was at RT lower than CAF (3.35 min), suggesting a compound with higher polarity, and two peaks were at RT higher than CAF (6.94 and 8.37 min, respectively), suggesting compounds less polar than CAF. The intense peak around 2.50 min was due to DMF, released by the cell junction; in fact, it was already present in the analyzed starting solution, and increased with electrolysis advancing. The PDA chromatograms of anolyte before, after 1 F and after 2 F anodic oxidation of CAF in ACN-H₂O are shown in Figure S2 (Supplementary Materials).

From the analysis of the pESI and/or nESI Total Ions Chromatograms (TIC), another peak at the lower RT 2.75 min was evidenced, not detectable in the PDA chromatogram because it was eluted under the large DMF peak. The characteristic molecular m/z value evidenced for each peak, in pESI and/or nESI, was extracted from the corresponding TIC to obtain peaks with high purity. The extracted chromatograms at the experimental m/z value (reported in Table 2) of the five peaks evidenced in the TIC in pESI and/or nESI are shown in Figure 2, where they have been reported according to the elution order, from bottom to top (a-f).

Table 2. Tentative assignation of anodic oxidation products of CAF in ACN 0.1 M Et₄NBF₄ containing 0.02 M water, at Pt electrodes, r.t., N₂ atmosphere, $E = +1.85$ V, vs. SCE.

Compound	RT (min)	M (Da) caltd	[M+H] ⁺ caltd/expt	[M-H] ⁻ caltd/expt	λ (nm)	Structure	Data in SM	2 F/1 F
1	2.75	250.09	251.10/251.22	-	294 ^a		Figure S3	+57%
2	3.35	188.09	[M+Na] ⁺ 211.08/211.06	187.08/187.09	203; 234		Figure S4	+71%
3	5.39	194.08	195.09/195.04	-	205; 272			-70%
4	6.94	213.07	-	212.07/212.03	220–240 ^b		Figure S5	+97%
5	8.37	228.09	229.09/229.10	-	209; 276		Figure S6	-28%

^a weak; ^b weak band in the range; caltd = calculated; expt = measured.

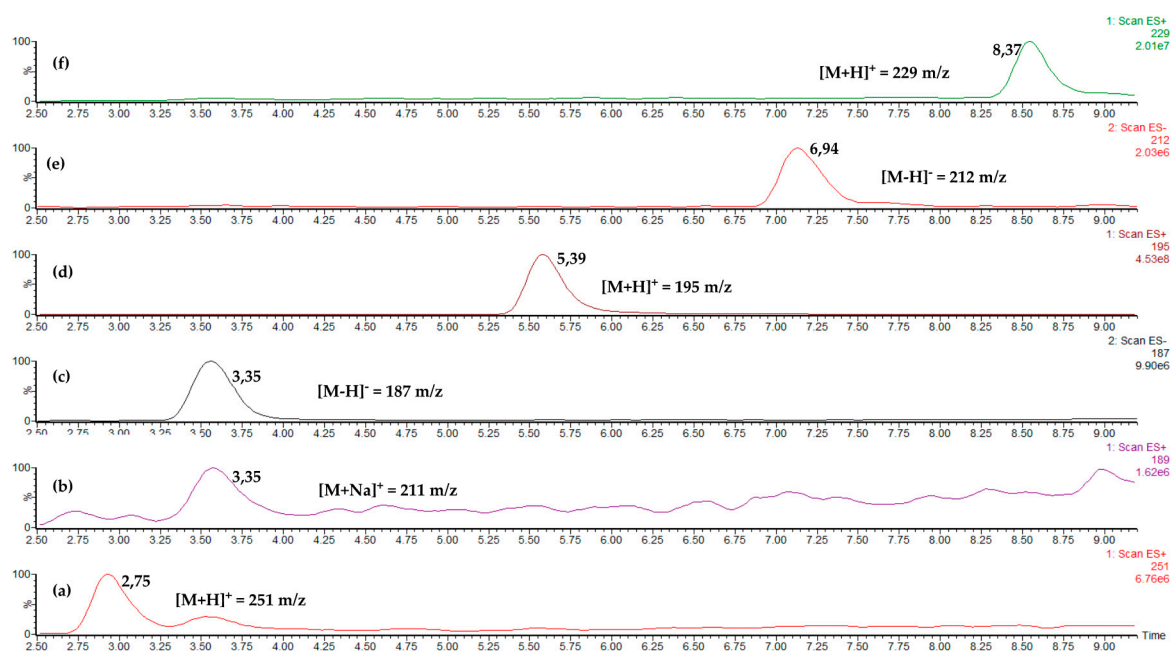


Figure 2. Chromatograms extracted from Total Ion Chromatograms (TIC) at the characteristic m/z value for each of the four analyzed peaks and CAF, reported in the elution order from bottom to top. Curve a: RT = 2.75 min, $[M+H]^+$ at m/z 251.22, compound 1 in Table 2; curve b: RT = 3.35 min, $[M+Na]^+$ at m/z 211.06; curve c: $[M-H]^-$ at m/z 187.09, compound 2 in Table 2; curve d: RT = 5.39 min, $[M+H]^+$ at m/z 195.04, CAF, compound 3 in Table 2; curve e: RT = 6.94 min, $[M-H]^-$ at m/z 212.03, compound 4 in Table 2; curve f: RT = 8.37 min, $[M+H]^+$ at m/z 229.10, compound 5 in Table 2. (a) compound 1; (b) compound 2 in ES+; (c) compound 2 in ES-; (d) compound 3; (e) compound 4; (f) compound 5.

The peaks of CAF (Figure 2d) obtained by extracting in pESI mode the $[M+H]^+$ value of 195.04 m/z from the TICs of anolyte, before starting electrolysis and after 2 F anodic oxidation, were integrated to evaluate the consumption of CAF, and a 14% of residual CAF after 2 F electrolysis was found, in agreement with voltammetric data (see Table 1). Data of CAF are included as compound 3 in Table 2.

Results for each of the other four peaks were reported according to the elution order, as follow.

The first peak, eluted at 2.75 min, was characterized by a $[M+H]^+$ value of m/z 251.22 (Table 2, Figure 2a) and an UV-vis spectrum with a very weak absorption with λ_{max} around 294 nm. The fragmentation profile evidenced a main fragment $[M+H-OH]^+$ with m/z 234.08 and other fragments corresponding to the loss of H_2O and $-NCH_3$. On the base of spectral data and elution order, the structure with molecular mass $M = 250.09$ Da reported as compound 1 in Table 2 has been proposed. UV-vis spectrum, pESI mass spectrum and pESI fragmentation pattern at two different collision energy (CE) values, are shown in Figure S3 (Supplementary Materials).

The second peak, eluted at 3.35 min, was characterized in pESI by a sodium adduct $[M+Na]^+$ value of m/z 211.06, and in nESI by a corresponding better evidenced $[M-H]^-$ value of m/z 187.09, evidence for the presence of an acidic H-atom in the structure. The fragmentation profile in pESI was characterized by the loss of H_2O while in nESI the loss of $-NH_2$ and $-NH_2CO$ was evidenced.

Absorptions at λ 203 nm and 234 nm were evidenced by the UV-vis spectrum. On the basis of spectral data and elution order, the structure with $M = 188.09$ Da reported as compound 2 in Table 2 has been proposed; UV-vis spectrum, pESI and nESI mass spectra and fragmentation patterns, at two different CE values in both nESI and pESI modes, are shown in Figure S4 (Supplementary Materials).

The fourth peak, eluted at 6.94 min, was characterized by a $[M-H]^-$ value of m/z 212.03 in nESI, suggesting the presence of an acidic H-atom in the structure. The fragmentation profile in nESI was characterized by a main fragment m/z 168.03, corresponding to a loss of 44 Da and likely due to the fragment $[M-H-CO_2]^-$. The UV-vis spectrum shows a weak absorption band in the range

of 220–240 nm. On the base of spectral data and elution order, the structure with $M = 213.07$ Da reported as compound **4** in Table 2 has been proposed. UV–vis spectrum, nESI mass spectrum and nESI fragmentation pattern at two different CE values are shown in Figure S5 (Supplementary Materials).

The fifth peak, eluted at 8.37 min, was characterized by a $[M+H]^+$ value of m/z 229.10 in pESI and an UV–vis spectrum with absorptions at 209 nm and 276 nm. The fragmentation profile in pESI was characterized by two main fragments with m/z 172.29 and 143.82, assigned to the loss of $-\text{CONCH}_3$ and the further loss of $-\text{CO}$, respectively. On the basis of spectral data and elution order, the structure with $M = 228.09$ Da reported as compound **5** in Table 2 has been proposed; UV–vis spectrum, pESI mass spectrum and pESI fragmentation pattern at two different CE values are shown in Figure S6 (Supplementary Materials).

In Table 2, the calculated monoisotopic molecular mass M , and both the calculated and the experimental values for $[M+H]^+$ and/or $[M-H]^-$ and/or $[M+Na]^+$ for each proposed structure have been reported.

4. Discussion

The electrochemical behavior of CAF has been in general sparingly studied, and the literature mainly reports studies in water, the story of CAF being strongly related to that of its corresponding uric acid: in fact, the anodic oxidation of CAF in water was proposed to involve the C^8 position of the imidazolic unit, on the basis of the methylated uric acid and its degradation products obtained after exhaustive electrolysis, with a whole four electrons process [26,27]. A bi-electronic anodic oxidation had been reported for uric acid, with the involvement of the $C^4 = C^5$ and a pathway towards high degradation products has been proposed [34]. 1,3,7-trimethyluric acid was also found after photooxidation of CAF in slightly alkaline solution [28].

The indirect electrochemical oxidation of CAF for environmental applications as removal of CAF from wastewater has been more recently reported, and the analysis of by-products was carried out by liquid chromatography-time of flight-mass spectrometry technique: the indirect oxidation of CAF was reported to involve other electrogenerated agents, such as hypochlorite [35].

In aprotic medium, the anodic oxidation of CAF was studied in strongly dry ACN: a mono-electronic process to form the radical cation $\text{CAF}^{\bullet+}$ was evidenced, and under these experimental conditions the caffeinium cation CAFH^+ was found as the only product, likely deriving by reaction of $\text{CAF}^{\bullet+}$ with a H-atom donor (Scheme, Equation (2)) [30].

In a previous work, the electrochemical behavior of CAF and TPh in aprotic medium was studied by cyclic voltammetry and UV–vis spectroelectrochemistry, joined by theoretical calculations [31]: a different behavior was found, and the N^7 atom was suggested making the difference. Experimental and theoretical data were in agreement with the one-electron oxidation, likely involving the $C^4 = C^5$ olefinic bond, to $\text{CAF}^{\bullet+}$. This latter was proposed to be quite stable in the case of the methylsubstituted- N^7 CAF, and to undergo fast deprotonation to the neutral radical in the case of the unsubstituted- N^7 TPh, with a different reactivity predictable for the neutral radical TPh^\bullet and the radical cation $\text{CAF}^{\bullet+}$.

A later study of the anodic oxidation of TPh evidenced the formation of dimeric forms of TPh, prevalently in organic solvents, supporting the neutral radical of TPh, but also the formation of highly oxidized products, prevalently in water [32].

The anodic oxidation of CAF, reported in the present work, has been studied to investigate on the reactivity of the $\text{CAF}^{\bullet+}$ in a proton-poor medium, as might occur to CAF under oxidative stress in a lipidic environment.

CAF has been oxidized at a Pt electrode until a 2 F current consumption, in both ACN and ACN containing 1 equivalent of water. A higher current efficiency was found in the presence of water: only 14% of the starting material was found in the final 2 F electrolyzed solution versus a 42% in ACN, as calculated by both HPLC-PDA-ESI-MS/MS and voltammetric data. Noteworthy is that the determination of CAF, eluted with solvents/formic acid 5mM and detected as CAFH^+ by pESI mode, provided the same percentage values calculated by cyclic voltammetric data, therefore

excluding CAFH^+ as an oxidation product under the present experimental conditions. A H-atom transfer (HT) reaction between a H-atom donor and $\text{CAF}^{\bullet+}$ might likely occur only under strongly dry conditions [30], or lipidic environment, while in the present work, the used ACN (HPLC grade) had a 0.02% nominal content of water, corresponding to about 10% of the starting amount of CAF.

Since the analysis of the electrolyzed solutions in ACN and ACN- H_2O evidenced a quite similar diode array (PDA) chromatographic profile, as shown in Figure S1, a and b, respectively, the structure of the oxidation products were investigated by chromatographic and spectral data relative to the electrolysis of CAF in ACN- H_2O . In fact, the main chromatographic peak, at lower RT (3.35 min, compound 2 in Table 2), was evidently due to a compound with polarity higher than CAF (RT = 5.39 min, compound 3 in Table 2), suggesting the presence of an oxygenated product of CAF in ACN- H_2O as well as in undried ACN, even if to a minimum extent ($\text{Area}_{(\text{CAF})}/\text{Area}_{(\text{peak } 2)} = 0.83$ in CAN vs. 0.70 in ACN- H_2O).

The mass spectral analysis evidenced a total of four main peaks besides CAF, as shown in Figure 2a–f, where the extracted TICs at each molecular peak value have been reported: two peaks were observed only in pESI (Figure 2a,f, respectively), one peak was observed only in nESI (Figure 2e) and another one was observed in both pESI and nESI modes (Figure 2b,c, respectively). The mass spectra of detected peaks excluded the presence of dimeric forms of CAF and/or de-methylated dimeric forms, unlike what was reported for the anodic oxidation of TPh under the same experimental conditions. This result supported the radical cation $\text{CAF}^{\bullet+}$, unable to undergo a subsequent proton transfer because of the methylated N^7 position: any coupling reaction following the primary anodic process could be therefore excluded.

The four chromatographic peaks were suggested to be due to compounds deriving from chemical reactions of the electrogenerated $\text{CAF}^{\bullet+}$ with a potential nucleophile present in the electrolyzed solution, likely water. All the chromatographic peaks were found increasing for advancing electrolysis except CAF and the named 5, in Table 2, whose intensity was found decreased after 2 F with respect to 1 F (Figure S2 and Table 2). This seemed to suggest 5 as a first reaction product of $\text{CAF}^{\bullet+}$ with water. The peak at 8.37 min was tentatively assigned to the 4,5-diol CAF derivative, structure 5 (Table 2): the UV–vis spectrum showed a characteristic λ_{max} at 276 nm, lightly shifted with respect to CAF, likely ascribed to the presence of bathochromic substituents offsetting the loss of the $\text{C}^4 = \text{C}^5$ conjugation [32]; the strong molecular peak, only in pESI, $[\text{M}+\text{H}]^+$ with m/z 229.10, was in agreement with the absence of acidic H-atom, and the fragmentation pattern was in agreement with the preserved methylxanthine structure, with the characteristic -57 fragment $[\text{M}+\text{H}-\text{CONCH}_3]^+$ [32] (Figure S6); last, the elution order was in agreement with a less polar structure, due to the possibility of intra-molecular H-bond.

The decreasing of this peak along the electrolysis (-28% from 1 F to 2 F, Table 2) suggested the transformation towards degradation product, namely compound 1 (Table 2). The peak at 2.75 min was tentatively assigned to the structure 1 on the base of the mass spectrum in pESI evidencing two strong peaks, $[\text{M}+\text{H}]^+$ at m/z 251.22 and $[\text{M}+\text{H}-\text{OH}]^+$ at m/z 234.08, and a complex fragmentation pattern consistent with the proposed structure (Figure S3); the possibility of intramolecular H-bond for the -NH function justified the absence of spectrum in nESI, and the -OH functions on the opened imidazolic unit explained well the very low RT (2.75 min, Table 2, Figure 2). Also, the loss of the xanthine characteristic absorption in the UV–vis spectrum agreed with the proposed structure 1.

The tentatively assigned structures 5 and 1 (1 being a degradation product of 5) strongly supported the anodic oxidation of $\text{C}^4 = \text{C}^5$ to $\text{CAF}^{\bullet+}$, the following nucleophilic attack by water to give the mono-substituted radical intermediate and its further easy oxidation at the same applied potential (evidenced by the doubling peak current intensity I in the presence of stoichiometric added water, Figure 1b, blue curve) to the final 4,5-diol derivative, in agreement with to the mechanism previously proposed [31]. Structure 5 had been also hypothesized in a study on the chemical degradation of CAF by HO^\bullet [29], but this is the first experimental evidence for the 4,5-diol derivative of CAF, at least up to our knowledge. A 4,5-diol derivative was also found among the anodic oxidation products of TPh [32].

The other two peaks were tentatively assigned to the structures 2 and 4 (Table 2), presenting the main difference of substitution on C⁸ position, with respect to compounds 1 and 5 discussed above.

The peak at RT 6.94 mn was assigned to structure 4, whose odd molecular mass 213.07 Da was in agreement with the loss of an N-atom from the original xanthine structure. The nESI spectrum was well justified by the acidic H-atom in C⁴, as well as the intense fragment [M-H-44]⁻ at m/z 168.03 was easily assigned to the loss of CO₂. 1,3,7-trimethyluric acid was not found in the electrolyzed solutions as well as the 4,5-diol- trimethyluric acid, as expected in agreement with studies on CAF in water that reported a proposed mechanism of slow oxidation to CAF uric acid, followed by fast oxidation to 4,5-diol CAF uric acid and a subsequent fast degradation process [26]. The proposed structure 4 might likely result from the same mono-substituted intermediate described above, giving a di-substituted derivative on C⁸ for resonance effect. A rearrangement by eliminating an -NH unit might lead to the final 4. A similar behavior was also found for a dimeric derivative of TPh [32].

The main chromatographic peak at RT 3.35 min, tentatively assigned to the structure 2 (Table 2), seemed to support what was discussed for 4. The UV-vis spectrum with λ_{max} at 234 nm was in agreement with the loss of the methylxanthine structure, whose characteristic λ_{max} is in the range of 272–276 nm [31,32]; the intense molecular peak in the nESI mass spectrum, [M-H]⁻ with m/z 187.09, and the weak but detectable ion in the pESI mass spectrum [M+Na]⁺ with m/z 211.06, were in agreement with the presence of an acidic H-atom (-N⁹H) and a carbonyl (-C⁸O) suitable for a sodium adduct [36], for a compound with molecular mass 188.09 Da; the fragmentation pattern in both pESI and nESI modes also strongly supported the proposed structure (Figure S4).

Noteworthy is that different kinds of degradation products seemed to occur for the 4,5-diol derivative 5 and the oxazolidin-2-one derivative 4, with the opening of the imidazolic unit (product 1) or the purinic unit (product 2), respectively.

5. Conclusions

The analysis of the products obtained by the anodic oxidation of caffeine under the controlled conditions of (i) applied potential and current as oxidant, (ii) water as reactant, and (iii) acetonitrile as friendly medium for mechanistic studies, has been described herein to get a further insight on the behavior of this natural widespread methylxanthine under oxidative conditions and on the reactivity of its radical cation, for useful synthetic applications in biomedical research as well as to shed light on its reactivity in a non-hydrophilic environment.

Electrolyses were carried out in undried ACN and ACN-H₂O; a higher current efficiency was found in ACN-H₂O, but a similar chromatographic profile was shown in both media. Four main products were evidenced by chromatographic separation followed by UV-vis spectrophotometric and mass spectrometric detection. Four corresponding structures have been tentatively assigned to the peaks on the base of elution order, mass spectrum in positive and/or negative electrospray ionization (pESI and/or nESI) recorded in full scan, fragmentation mass spectrum recorded in pESI and/or nESI by selecting the molecular mass evidenced for each peak as parent ion before entering the collision cell at different collision energy values, and UV-vis spectrum. A 4,5-diol derivative 5 and an oxazolidin-2-one derivative 4 were proposed as assigned structures, well supported by all experimental data. Both products well supported the mechanism previously proposed [31] regarding the primary anodic oxidation of the methylxanthine olefinic C⁴ = C⁵ bond. Two highly polar degradation products were also found, whose proposed structures 1 and 2 were well supported by all experimental data. Compound 1, characterized by the opening of the imidazolic unit, was suggested originating from the 4,5-diol derivative 5, while compound 2, characterized by the opening of the purinic unit, was suggested originating from the oxazolidin-2-one derivative 4. These results offer an interesting new insight on the reactivity of the radical cation of CAF, for useful synthetic applications and a better understanding of the behavior of CAF under stress oxidative conditions.

Supplementary Materials: The following are available online at <http://www.mdpi.com/2673-3293/1/1/5/s1>, Figure S1: ACN vs. ACN-H₂O; Figure S2: ACN-H₂O; Figure S3: Compound 1; Figure S4: Compound 2; Figure S5: Compound 4; Figure S6: Compound 5.

Author Contributions: All authors contributed equally to this manuscript. All authors have read and agreed to the published version of the manuscript.

Funding: This research was supported by Sapienza University of Rome (Project N. RM11916B462FA71F).

Acknowledgments: The authors want to thank Marco Di Pilato for technical support.

Conflicts of Interest: The authors declare no conflict of interest.

References

1. Shechter, M.; Shalmon, G.; Scheinowitz, M.; Koren-Morag, N.; Feinberg, M.S.; Harats, D.; Sela, B.A.; Sharabi, Y.; Chouraqui, P. Impact of acute caffeine ingestion on endothelial function in subjects with and without coronary artery disease. *Am. J. Cardiol.* **2011**, *107*, 1255–1261. [[CrossRef](#)] [[PubMed](#)]
2. Gaytan, S.P.; Pasaro, R. Neonatal caffeine treatment up-regulates adenosine receptors in brainstem and hypothalamic cardio-respiratory related nuclei of rat pups. *Exp. Neurol.* **2012**, *237*, 247–259. [[CrossRef](#)] [[PubMed](#)]
3. Barrès, R.; Yan, J.; Egan, B.; Trebak, J.T.; Rasmussen, M.; Fritz Caidahl, K.; Krook, A.; O’Gorman, D.J.; Zierath, J.R. Acute exercise remodels promoter methylation in human skeletal muscle. *Cell Metab.* **2012**, *15*, 405–411. [[CrossRef](#)] [[PubMed](#)]
4. Wardle, M.C.; Treadway, M.T.; de Wit, H. Caffeine increases psychomotor performance on the effort expenditure for rewards task. *Pharmacol. Biochem. Behav.* **2012**, *102*, 526–531. [[CrossRef](#)]
5. Ward, N.; Whitney, C.; Avery, D.; Dunner, D. The analgesic effects of caffeine in headache. *Pain* **1991**, *44*, 151–155. [[CrossRef](#)]
6. Renner, B.; Clarke, G.; Grattan, T.; Beisel, A.; Muller, C.; Werner, U.; Kobal, G.; Brune, K. Caffeine accelerates absorption and enhances the analgesic effect of acetaminophen. *J. Clin. Pharmacol.* **2007**, *47*, 715–726. [[CrossRef](#)] [[PubMed](#)]
7. Monteiro, J.; Alves, M.G.; Oliveira, P.F.; Silva, B.M. Pharmacological potential of methylxanthines: Retrospective analysis and future expectations. *Crit. Rev. Food Sci. Nutr.* **2019**, *59*, 2597–2625. [[CrossRef](#)]
8. Prasanthi, J.R.P.; Dasari, B.; Marwarha, G.; Larson, T.; Chen, X.; Geiger, J.D.; Ghribi, O. Caffeine protects against oxidative stress and Alzheimer’s disease-like pathology in rabbit hippocampus induced by cholesterol-enriched diet. *Free Radic. Biol. Med.* **2010**, *49*, 1212–1220. [[CrossRef](#)]
9. Devasagayam, T.P.A.; Kamat, J.P.; Mohan, H.; Kesavan, P.C. Caffeine as an antioxidant: Inhibition of lipid peroxidation induced by reactive oxygen species. *Biochim. Biophys. Acta* **1996**, *1282*, 63–70. [[CrossRef](#)]
10. Varma, S.D.; Hegde, K.R. Kynurenine-induced photo oxidative damage to lens in vitro: Protective effect of caffeine. *Mol. Cell. Biochem.* **2010**, *340*, 49–54. [[CrossRef](#)]
11. León-Carmona, J.R.; Galano, A. Is Caffeine a Good Scavenger of Oxygenated Free Radicals? *J. Phys. Chem.* **2011**, *115*, 4538–4546. [[CrossRef](#)] [[PubMed](#)]
12. Brezová, V.; Šlebodová, A.; Staško, A. Coffee as a source of antioxidants: An EPR study. *Food Chem.* **2009**, *114*, 859–868. [[CrossRef](#)]
13. Załuski, M.; Schabikowski, J.; Schlenk, M.; Olejarz-Maciej, A.; Kubas, B.; Karcz, T.; Kuder, K.; Latacz, G.; Zygmunt, M.; Synak, D.; et al. Novel multi-target directed ligands based on annelated xanthine scaffold with aromatic substituents acting on adenosine receptor and monoamine oxidase B. Synthesis, in vitro and in silico studies. *Bioorg. Med. Chem.* **2019**, *27*, 1195–1210. [[CrossRef](#)] [[PubMed](#)]
14. Singh, N.; Kumar Shreshtha, A.; Thakur, M.S.; Patra, S. Xanthine scaffold: Scope and potential in drug development. *Heliyon* **2018**, *4*, e00829. [[CrossRef](#)]
15. Załuski, M.; Stanuch, K.; Karcz, T.; Hinz, S.; Latacz, G.; Szymańska, E.; Schabikowski, J.; Doróż-Płonka, A.; Handzlik, J.; Drabczyńska, A.; et al. Tricyclic xanthine derivatives containing a basic substituent: Adenosine receptor affinity and drug-related properties. *Med. Chem. Commun.* **2018**, *9*, 951–962. [[CrossRef](#)]
16. Kascatan-Nebioglu, A.; Melaiye, A.; Hindi, K.; Durmus, S.; Panzner, M.J.; Hogue, L.A.; Mallett, R.J.; Hovis, C.E.; Coughenour, M.; Crosby, S.D.; et al. Synthesis from Caffeine of a Mixed N-Heterocyclic Carbene-Silver Acetate Complex Active against Resistant Respiratory Pathogens. *J. Med. Chem.* **2006**, *49*, 6811–6818. [[CrossRef](#)]

17. Pandolfi, F.; Chiarotto, I.; Mattiello, L.; Rocco, D.; Feroci, M. Cathodic reduction of caffeine: Synthesis of an amino-functionalized imidazole from a biobased reagent. *Synlett* **2019**, *30*, 1215–1218. [[CrossRef](#)]
18. Pandolfi, F.; Mattiello, L.; Zane, D.; Feroci, M. Electrochemical behaviour of 9-methylcaffeinium iodide and in situ electrochemical synthesis of hymeniacidin. *Electrochim. Acta* **2018**, *280*, 71–76. [[CrossRef](#)]
19. Pandolfi, F.; Chiarotto, I.; Mattiello, L.; Petrucci, R.; Feroci, M. Two Different Selective Ways in the Deprotonation of β -Bromopropionanilides: β -Lactams or Acrylanilides Formation. *ChemistrySelect* **2019**, *4*, 12871–12874. [[CrossRef](#)]
20. Murthy, P.S.; Naidu, M.M. Sustainable management of coffee industry by-products and value addition. A review. *Resour. Conserv. Recycl.* **2012**, *66*, 45–58. [[CrossRef](#)]
21. Švorc, L. Determination of caffeine: A comprehensive review on electrochemical method. *Int. J. Electrochem. Sci.* **2013**, *8*, 5755–5773.
22. Trani, A.; Petrucci, R.; Marrosu, G.; Zane, D.; Curulli, A. Selective electrochemical determination of caffeine at a gold-chitosan nanocomposite sensor: May little change on nanocomposites synthesis affect selectivity? *J. Electroanal. Chem.* **2017**, *788*, 99–106. [[CrossRef](#)]
23. Trani, A.; Petrucci, R.; Marrosu, G.; Curulli, A. Determination of Caffeine @ Gold Nanoparticles Modified Gold (Au) Electrode: A Preliminary Study. *Sensors* **2015**, *319*, 147–151. [[CrossRef](#)]
24. Lovecchio, N.; Costantini, F.; Nascetti, A.; Petrucci, R.; de Cesare, G.; Caputo, D. Development of an Electrochemiluminescence-based Lab-on-Chip Using Thin/Thick Film Technologies. In Proceedings of the 8th International Workshop on Advances in Sensors and Interfaces, IWASI 2019, Otranto, Italy, 13–14 June 2019; pp. 79–83.
25. Petrucci, R.; Chiarotto, I.; Mattiello, L.; Passeri, D.; Rossi, M.; Zollo, G.; Feroci, M. Graphene Oxide: A Smart (Starting) Material for Natural Methylxanthines Adsorption and Detection. *Molecules* **2019**, *24*, 4247. [[CrossRef](#)] [[PubMed](#)]
26. Hansen, B.H.; Dryhurst, G. Electrochemical oxidation of theobromine and caffeine at the pyrolytic graphite electrode. *Electroanal. Chem. Interfacial Electrochem.* **1971**, *30*, 407–416. [[CrossRef](#)]
27. Hansen, B.H.; Dryhurst, G. Voltammetric oxidation of some biologically important xanthines at the pyrolytic graphite electrode. *Electroanal. Chem. Interfacial Electrochem.* **1971**, *30*, 417–426. [[CrossRef](#)]
28. Kumar, M.R.; Adinarayana, M. Oxidation of caffeine by phosphate radical anion in aqueous solution under anoxic conditions. *Proc. Indian Acad. Sci. Chem. Sci.* **2000**, *112*, 551–557. [[CrossRef](#)]
29. Dalmázio, I.; Santos, L.S.; Lopes, R.P.; Eberlin, M.N.; Augusti, R. Advanced Oxidation of Caffeine in Water: On-line and Real-Time Monitoring by Electrospray Ionization Mass Spectrometry. *Environ. Sci. Technol.* **2005**, *39*, 5982–5988. [[CrossRef](#)]
30. Chan, K.K.; Ganguly, R.; Li, Y.; Webster, R.D. Electrochemically Controlled One-Electron Oxidation Coupled to Consecutive Hydrogen Atom Transfer of Caffeine. *ChemElectroChem* **2014**, *1*, 1557–1562. [[CrossRef](#)]
31. Petrucci, R.; Zollo, G.; Curulli, A.; Marrosu, G. A new insight into the oxidative mechanism of caffeine and related methylxanthines in aprotic medium: May caffeine be really considered as an antioxidant? *BBA Gen. Subj.* **2018**, *1862*, 1781–1789. [[CrossRef](#)]
32. Chiarotto, I.; Mattiello, L.; Pandolfi, F.; Rocco, D.; Feroci, M.; Petrucci, R. Electrochemical oxidation of theophylline in organic solvents: HPLC-PDA-ESI-MS/MS analysis of the oxidation products. *ChemElectroChem* **2019**, *6*, 4511–4521. [[CrossRef](#)]
33. Feroci, M.; Civitarese, T.; Pandolfi, F.; Petrucci, R.; Rocco, D.; Zane, D.; Zollo, G.; Mattiello, L. Electrochemical Studies of New Donor-Acceptor Oligothiophenes. *ChemElectroChem* **2019**, *6*, 4016–4021. [[CrossRef](#)]
34. Struck, W.A.; Elving, P.J. Electrolytic oxidation of uric acid: Products and mechanism. *Biochemistry* **1965**, *4*, 1343–1353. [[CrossRef](#)] [[PubMed](#)]
35. Al-Qaim, F.F.; Mussa, Z.H.; Othman, M.R.; Abdullah, M.P. Removal of caffeine from aqueous solution by indirect electrochemical oxidation using a graphite-PVC composite electrode: A role of hypochlorite ion as an oxidizing agent. *J. Hazard. Mater.* **2015**, *300*, 387–397. [[CrossRef](#)] [[PubMed](#)]
36. Panusa, A.; Petrucci, R.; Lavecchia, R.; Zuurro, A. UHPLC-PDA-ESI-TOF/MS metabolic profiling and antioxidant capacity of arabica and robusta coffee silverskin: Antioxidants vs phytotoxins. *Food Res. Inter.* **2017**, *99*, 155–165. [[CrossRef](#)]

